Modeling of radial well lateral screens using 1D finite elements

M. Dimkic, V. Rankovic, N. Filipovic, B. Stojanovic, V. Isailovic, M. Pusic and M. Kojic

ABSTRACT

A water supply system including radial wells (RWs) is usually large, extending several tens of kilometers horizontally and is dozens of meters deep. An RW is a vertical shaft with lateral screens, which radially penetrate the soil. A large and complex 3D finite element (FE) mesh also needs to include laterals with cross-sectional dimensions measured in centimeters. An adequate representation of lateral screens by line elements, with nodes coinciding with the 3D FE mesh nodes, is desirable in order to simplify modeling, render the computation efficient, and present the results in an easily readable form. Line elements are introduced for the lateral screens and accuracy of the results is analyzed. It was found that the domain size of an RW (or laterals) has a more pronounced effect on accuracy than mesh density. The authors' conclusion is that the concept of 1D RW lateral screens representation is adequate for practical purposes.

Key words | 1D representation of laterals, finite elements, groundwater flow, radial well lateral screens, radial wells

M. Dimkic
M. Pusic
Jaroslav Cerni Institute for the Development of Water Resources, Jaroslava Cernog 80, 11226 Belgrade, Serbia

V. Rankovic (corresponding author)
N. Filipovic
B. Stojanovic
V. Isailovic
M. Kojic
University Metropolitan Belgrade – Research and Development Center for Bioengineering BioIRC, Prvoslava Stojanovica 6, 34000 Kragujevac, Serbia
E-mail: *vladar@kg.ac.rs*

N. Filipovic
University of Kragujevac, Faculty of Engineering, Sestre Janjic 6, 34000 Kragujevac, Serbia

M. Pusic
University of Belgrade, Faculty of Mining and Geology, Djusina 7, 11000 Belgrade, Serbia

B. Stojanovic
University of Kragujevac, Faculty of Science, Radoja Domanovica 12, 34000 Kragujevac, Serbia

V. Rankovic
University of Kragujevac, Faculty of Economics, Djure Pucara 3, 34000 Kragujevac, Serbia

INTRODUCTION

Radial wells (RWs) installed by directional drilling can improve the characteristics of a water supply to treatment plants. They are usually placed in high-conductivity sand and gravel sediments beneath rivers. Water then flows from the river to the RW through the sand and gravel in the riverbed, where the concentration of suspended solids and dissolved micropollutants is reduced by filtration and dilution with groundwater (Ray *et al.* 2002). This decreases the cost of final treatment and/or improves the ultimate water quality. An important step in evaluating the application of this technology is to predict the flow rates available from the RWs.

A groundwater flow analysis provides the spatial fields of flow potential (pressure) and fluid velocity for a given set of boundary conditions. In general, these physical fields are functions of time. For fluid flow through a porous medium at low velocities, Darcy's law is considered fundamental. Based on this law and the continuity equation for fluids, the basic differential equation for steady-state and non-steady-state problems can be derived.

The flow regions of a real water supply system based on RWs are large (kilometers wide and dozens of meters deep). The flow is truly 3D, with complex boundary conditions, such as a water table or river, which are variable over

doi: 10.2166/hydro.2012.008

time. Complexity is significantly increased by the non-homogeneity of the porous soil, with layers whose conductivities can differ by several orders of magnitude. The layers can be geometrically irregular and have different thickness. In addition to these complexities, the RWs themselves represent singularity-type concentrated domains with high flow gradients in their vicinity. An RW is a long vertical shaft which has several (usually eight) lateral screens, or drains at the bottom, penetrating the soil in radial directions. RW lateral screens represent a set of pipes with slots distributed along the screen circumference (perforated pipe). Water flows into the lateral screen from the surrounding soil through the slots and into the bottom of the RW.

During the exploitation period the rate of ground water inflow decreases. This is because a layer of low-conductivity soil usually develops around the screens. Very often this phenomenon is called well ageing. Well ageing causes yield decrease of the whole groundwater source and therefore water supply, so that after some period of exploitation groundwater source must be renewed. Renewal process can be realized by cleaning the existing screens, by closing the existing and injecting of new ones, or by generation of new RWs.

Computer modeling is very useful in the analysis of the existing water source, in predicting its performance and in planning its renewal. Using numerical analysis of the ground water flow in the screen's vicinity, the hydrology engineer can decide what type of renewal is the most efficient. Also, in the case that the best solution is injection of new screens, numerical simulations can provide optimal solution for each screen implementation.

A number of authors have developed numerical or analytical models of groundwater flow into a horizontal well. Huisman (1972) and Strack (1989) developed analytic solutions for 2D flow to radial collector wells. Using the boundary integral equation method, Bischoff (1981) developed a model of 3D flow to a collector well with three lateral arms in a confined aquifer subjected to uniform flow. A 3D analytical solution for a horizontal well (in essence one arm of a collector well) in a confined aquifer was formulated by Steward & Jin (2001). Semi-analytic solutions based on Laplace transforms for 3D flow to horizontal wells in unconfined and leaky aquifers were introduced by Zhan & Zlotnik (2002) and Zhan & Park (2003).

One of the first numerical models of a collector well was introduced by Ophori & Farvolden (1985). They initially used a one-layer finite element (FE) model and later replaced the collector well by three point sinks. Eberts & Bair (1990) modeled regional flow to four collector wells in Columbus, Ohio. They used a two-aquifer MODFLOW model and represented each collector by one grid cell of size 1,000 by 1,000 feet (304.8 by 304.8 meters). Chen *et al.* (2003) developed a polygon finite-difference model of a horizontal well. The flow inside the screen was approximated by a flow through an equivalent porous medium. The hydraulic conductivity of the porous medium was defined as a function of the flow rate in the screen. More recently, Chen & Zhang (2009) presented well models for 2D flow using different numerical methods such as a standard FE method, control volume FE, and mixed FE methods.

Considering FE modeling of RW lateral screens, it is possible to generate a very fine mesh of 3D FEs with a boundary at the lateral screen's surface. This very fine mesh must be compatible with the course mesh of the flow domain. Because of very complex geometry of soil layers and irregular spreading of screens through the porous soil, generation of a full 3D mesh requires significant effort. This implies that the engineer has to model each screen manually spending many engineer-hours for every computer model. Also, very fine mesh is necessary in the vicinity of each well screen so that the number of FEs and computational time are drastically increased with the number of screens.

In order to overcome the problem of RW lateral screens inclusion in a numerical 3D flow model, Luther & Haitjema (2000) developed a solution based on single layer Dupuit-Forchheimer (2D) analytic element model. Analytic element models are used to enforce boundary conditions on the phreatic surface and seepage faces at vertical wells, and to maintain fixed-head boundary conditions. These analytic models do not employ a computational grid, but directly represent the laterals using line-sinks. Bakker *et al.* (2005) introduced a multi-layer analytic element model in order to simulate 3D flow near radial collector wells. They modeled the aquifer as a set of horizontal layers. Resistance to vertical flow in the aquifer is modeled as the resistance between horizontal layers. More recently, Haitjema *et al.* (2010) developed a Cauchy boundary condition along a horizontal well in a Dupuit-Forchheimer model. They presented a solution

which includes lateral screens in a regional Dupuit-Forchheimer model by applying the Cauchy boundary condition on an arrangement of equivalent fictitious streams.

It would be an important benefit if the lateral screens could be represented by line FEs with nodes coinciding with those of the 3D mesh generated for the whole flow domain. This study offers a 3D–1D FE model, where the line elements have characteristics which adequately substitute a detailed 3D model of RW lateral screens.

The accuracy of the solutions obtained by introducing 1D representation of RW lateral screen was investigated by comparing the solutions obtained from detailed 3D models and the 3D–1D models. Two examples which reflect typical cases encountered in engineering practice are used for accuracy assessment, and one where our 3D–1D model is implemented to a real water supply system.

The paper is organized as follows: the next section presents the basic relations for the 1D elements which appropriately substitute a 3D detailed model, followed by examples for the accuracy assessment of this 1D substitution, and its applicability to real engineering problems. Finally, in the concluding remarks the authors emphasize that the proposed relatively simple concept is generally applicable in this area of engineering.

THEORETICAL BACKGROUND

In this section, a brief theoretical background for modeling of fluid flow through porous media is given. Then, a derivation of basic relations of 1D FEs as models of RW lateral screens with appropriate characteristics is presented.

Description of a radial well

An RW generally comprises of a vertical concrete shaft, with a depth of several dozen meters and a radius between 4 and 5 m (Figure 1). Holes are drilled into the lower section of the shaft, usually eight, through which horizontal lateral screens are inserted into the aquifer. The laterals are perforated pipes, through which groundwater enters the well. The length of the lateral screens is usually 40–50 m, and the radius is 0.1–0.3 m.

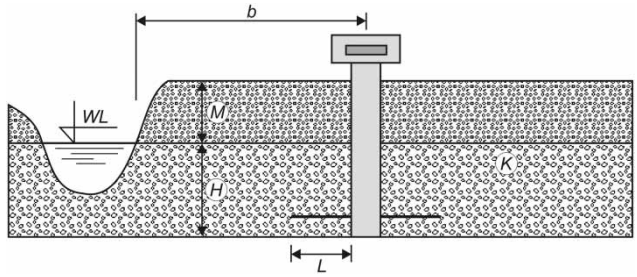

Figure 1 | Physical model of a radial well. There are two layers of soil (unsaturated – above the river water level *WL*, and saturated – below the river water level, with conductivity *K*), whose heights are *M* and *H*, respectively, so the depth of the well is approximately $M + K$; *L* is the length of the RW lateral screens and *b* is the distance of the RW from the river bank.

Modeling of fluid flow through a porous medium

The basic parameter in the modeling of fluid flow through a porous medium is the potential ϕ defined as

$$\phi = \frac{p}{\gamma} + h \tag{1}$$

where p is the fluid pressure, γ is the specific weight, and h is the height in the vertical direction measured with respect to an adopted reference plane. Fluid velocity $\mathbf{q}$, also known as Darcy's velocity, represents the fluid volume which passes over unit time through a unit area of the porous medium. This velocity is related to the potential as

$$\mathbf{q} = -\mathbf{K}\nabla\phi \tag{2}$$

where $\mathbf{K}$ is the diagonal conductivity matrix. Then, the continuity equation for non-steady-state conditions can be written as

$$k_x \frac{\partial^2\phi}{\partial^2 x} + k_y \frac{\partial^2\phi}{\partial^2 y} + k_z \frac{\partial^2\phi}{\partial^2 z} + Q = S\frac{\partial\phi}{\partial t} \tag{3}$$

where k_x, k_y, k_z are coefficients of the matrix $\mathbf{K}$, Q is the volumetric flux, and S is the storage.

If there is a water surface, the points at which the condition

$$\phi \geq h \tag{4}$$

is satisfied are points on or below the water surface. General formulation of the conductivity matrix can be written as

$$\mathbf{K} = (1-\alpha)\mathbf{K}^0,\ \alpha = \begin{Bmatrix} 0, & \varphi \geq h \\ 0.999 & \varphi < h \end{Bmatrix} \tag{5}$$

where the matrix $\mathbf{K}^0$ is the matrix for points below the water surface.

The balance equation for a (3D) FE in the case of an incremental-iterative scheme (for non-steady-state conditions with a water surface, with conductivity coefficients dependent on potential) can be written as (Dimkic *et al.* 2007a, b; Dimkic & Pusic 2008; Pusic & Dimkic 2008)

$$\left({}^{t+\Delta t}\mathbf{K}^e_{\phi\phi} + \frac{1}{\Delta t}\,{}^{t+\Delta t}\mathbf{S}^e\right)^{(i-1)} \Delta\underline{\phi}^{e(i)} = {}^{t+\Delta t}\mathbf{f}^{e(i-1)}_{\phi} \tag{6}$$

where

$${}^{t+\Delta t}\mathbf{K}^e_{\phi\phi} = \int_V \left[{}^{t+\Delta t}k_x \frac{\partial \mathbf{H}^T_\phi}{\partial x}\frac{\partial \mathbf{H}_\phi}{\partial x} + {}^{t+\Delta t}k_y \frac{\partial \mathbf{H}^T_\phi}{\partial y}\frac{\partial \mathbf{H}_\phi}{\partial y} + {}^{t+\Delta t}k_z \frac{\partial \mathbf{H}^T_\phi}{\partial z}\frac{\partial \mathbf{H}_\phi}{\partial z}\right] \mathrm{d}V \tag{7}$$

$${}^{t+\Delta t}\mathbf{S}^e = -\int_A {}^{t+\Delta t}S\mathbf{H}^T_\phi \mathbf{H}_\phi \mathrm{d}V \tag{8}$$

Here $\mathbf{H}_\phi$ is the interpolation matrix (with dimensions $1 \times N$, where N is number of element nodes), Δt is the time step, and $\Delta\underline{\phi}^{e(i)}$ is the vector of increments of nodal potentials. The vector ${}^{t+\Delta t}\mathbf{f}^{e(i-1)}_{\phi}$ depends on the solution of the previous iteration and on volumetric and surface fluxes. The indices $t+\Delta t$ and 'i' indicate the end of a time step and the iteration counter within the time step, respectively.

1D FE is introduced for modeling RW lateral screens, for which the element matrix is:

$${}^{t+\Delta t}\mathbf{K}^e_{\phi\phi} = \int_L {}^{t+\Delta t}k_x \frac{\partial \mathbf{H}^T_\phi}{\partial x}\mathrm{d}L \tag{9}$$

where L is the element length. It is assumed that the conductivities depend on the potential (as in Equation (5)), hence the left upper index $t+\Delta t$ of the conductivity coefficients refers to their values for the potential ${}^{t+\Delta t}\phi$.

Equivalent-line finite element for radial well lateral screen

As stated in the above description of RW lateral screens, the screen cross-sectional dimensions are smaller than their length by an order of magnitude. The actual water flow consists of a radial portion through the slots of the lateral's wall and an axial portion along the lateral. In a representation of the laterals by 1D FEs, the axial flow can be modeled using the conductivity matrix given in Equation (9), with a high conductivity coefficient k_x. The nodes of line FEs are then placed to coincide with 3D mesh nodes and the 1D and 3D elements are coupled with common nodes in a standard manner. However, radial flow is rather complex for modeling because a relatively thin layer of soil, the so-called colmated layer of low conductivity, develops over time. This thin layer is crucial for overall lateral screen performance.

In order to incorporate the conductivity of the colmated layer into the FE model, radial line elements are introduced at each FE node of the lateral screen line, with properties that adequately represent the conductivity characteristics of the colmated material around the lateral's wall. The concept of this lateral screen representation is shown in Figure 2. It is first assumed that the lateral screen lies between the mesh lines for easier presentation of the concept.

The lateral screen, whose internal diameter is d_0 and which is surrounded by a colmated layer of variable thickness, lies between the 3D mesh lines and is displaced by the radial elements. The potentials for segments along the axis of the lateral screen are $\Phi^{\mathrm{int}}_1, \Phi^{\mathrm{int}}_2, \ldots.., \Phi^{\mathrm{int}}_N$ inside the screen, while the corresponding potentials of the surrounding material are $\Phi^{\mathrm{ext}}_1, \Phi^{\mathrm{ext}}_2, \ldots.., \Phi^{\mathrm{ext}}_N$. The lengths of the line FEs along the lateral screen axis are $l_{a1}, l_{a2}, \ldots, l_{aN}$; and the lengths of the radial line elements are $l_{r1}, l_{r2}, \ldots, l_{rN}$. The conductivities of the radial elements are $k_1, k_2, \ldots, k_N$.

The following assumptions are made (in accordance with Figure 2):

1. the conductivity and the thickness of the colmated layer along a lateral screen segment (screen FE) are constant;
2. the potential gradient (in radial direction of the segment) in the colmated layer along the lateral screen segment is constant; and
3. for given potentials Φ^{ext}_i and Φ^{int}_i at a segment 'i' , the radial flow rate through the screen surface is equal to the flow rate through the equivalent radial line element.

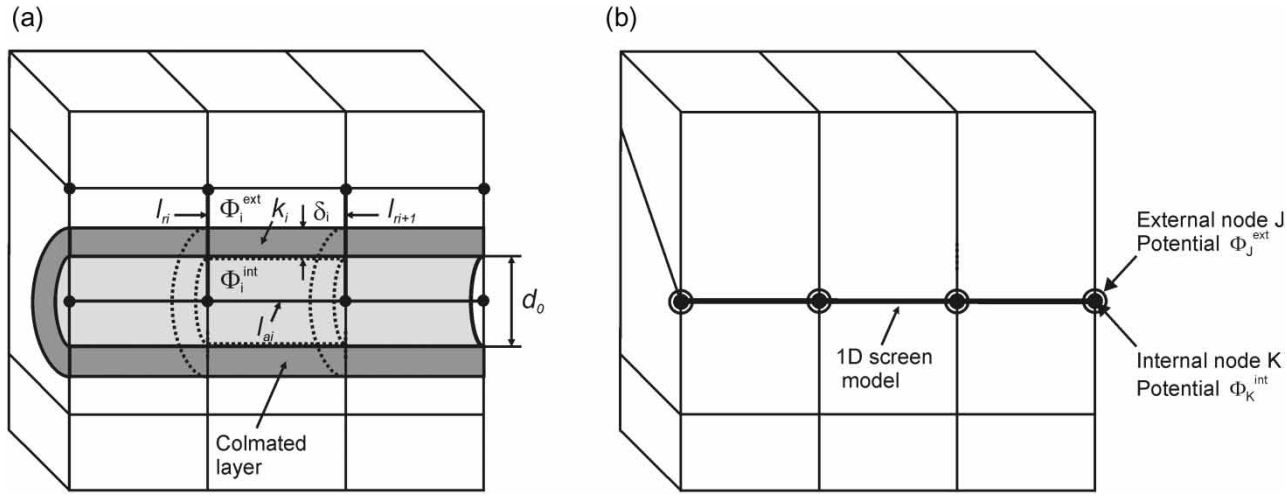

Figure 2 | Lateral screen modeling concept, using line elements: (a) Geometry of the RW lateral screen, with the screen displaced by radial element lengths l_{ri}; (b) 1D representation of the lateral screen (line elements coincide with the 3D mesh, external nodes have potential of the surrounding soil, while the internal nodes have potential of the screen interior).

In order to derive the equivalent conductivity for a radial element, Darcy's equation in the radial direction is used:

$$v_r = k_{\text{kol}} \frac{\mathrm{d}\Phi}{\mathrm{d}r} \tag{10}$$

where k_{kol} is conductivity of the colmated layer and v_r is the velocity in the radial direction. The radial flow rate (mass flux) for the lateral screen segment, with length l_{ai} and thickness δ_i, is:

$$Q_i = k_{\text{kol}(i)} \left(\frac{\mathrm{d}\Phi}{\mathrm{d}r}\right)_i^{\text{ext}} l_{ai}(d_0+\delta_i)\pi \tag{11}$$

where $(\mathrm{d}\Phi/\mathrm{d}r)^{\text{ext}}$ corresponds to the external lateral screen surface. The radial gradient of the potential can be expressed as $(\mathrm{d}\Phi/\mathrm{d}r)_i^{\text{ext}} = \Delta\Phi_i/\delta_i$, so that the above expression transforms into:

$$Q_i = k_{\text{kol}(i)} \frac{\Delta\Phi_i}{\delta_i} l_{ai}(d_0+\delta_i)\pi \tag{12}$$

The flow rate through the radial line element which has the potential difference $\Delta\Phi_i$ $(= \Phi_i^{\text{ext}} - \Phi_i^{\text{int}})$ is:

$$Q_{ri} = k_i \frac{\Delta\Phi}{l_{ri}} A_i = \overline{K_i}\Delta\Phi \tag{13}$$

where k_i is the conductivity, A_i is the cross-sectional area, l_{ri} is the length, and $\overline{K_i}$ is the equivalent conductivity of the radial 1D element. By equating the flow rate from the last two equations, the equivalent conductivity of the 1D element is obtained for the segment (line FE) of the lateral:

$$\overline{K_i} = k_{\text{kol}(i)} \frac{l_{ai}}{\delta_i}(d_0+\delta_i)\pi \tag{14}$$

Now, we can write the balance equation for radial line element i (according to Equation (6)) as:

$$\bar{K}_i \begin{bmatrix} 1 & -1 \\ -1 & 1 \end{bmatrix} \begin{bmatrix} \Delta\Phi_i^{\text{ext}} \\ \Delta\Phi_i^{\text{int}} \end{bmatrix} = \begin{bmatrix} Q_i^{\text{ext}} \\ Q_i^{\text{int}} \end{bmatrix} \tag{15}$$

for any equilibrium iteration. It is important that the conductivity of the radial element does not depend on the length of the element, so that it can be a zero-length element. Therefore, for each screen segment there is an element with two nodes on the segment, one having the potential at the lateral screen surface, and the other with the potential at the axis of the screen.

Since the nodes of the FE mesh must be connected, one radial element is associated with the zero-length at each node along the lateral screen axis. The nodes of the lateral screen are then doubled (see Figure 2(b)), coinciding spatially, one corresponding to the external surface of the screen (and therefore to the surrounding soil), and the other representing the screen interior. The flow rate associated with the radial element at node J takes half of the

flow rates of the adjacent segments i and $(i-1)$, i.e.

$$Q_{rJ} = 0.5(Q_{i-1} + Q_i) \tag{16}$$

from which the equivalent conductivity follows:

$$\overline{K}_j = \frac{k_{\mathrm{kol}(i-1)} l_{a(i-1)} (d_0 + \delta_{i-1})\pi}{2\delta_{i-1}} + \frac{k_{\mathrm{kol}(i)} l_{ai} (d_0 + \delta_i)\pi}{2\delta_i} \tag{17}$$

VERIFICATION EXAMPLES

In this section, two models are used for accuracy assessment of the proposed 1D representation of RW lateral screens. The first example is the model of a cylindrical domain, while a square shape (rectangular prism) domain is addressed in the second example. Accuracy is specified by comparing the results obtained from a detailed 3D model (hereafter: 3D model) and implementing line radial elements (hereafter: 1D model). Finally, a model of a real engineering problem is presented to demonstrate applicability of our simple and efficient 3D–1D coupling concept.

The proposed algorithm has been implemented in the FE software package PAK-P (Kojic *et al.* 1998) coded in FORTRAN 90, which has been verified in numerous applications. We used in-house developed graphical pre-and post-processor Lizza (Dimkic *et al.* 2009) coded in C++. The calculations were performed on personal computer with Intel Core™2 Duo CPU E7300 2.66GHz processor, 2GB of RAM and Windows XP OS.

Cylindrical domain

A cylindrical domain belonging to an RW lateral screen is used to examine the accuracy of 1D representation of the lateral screen. The hole along the axis of the cylinder with radius of 0.25 m (R_{screen}) represents a screen (Figure 3). The thickness of the cylinder is 15 m (L). The conductivity coefficient for the entire cylinder is $K = 10^{-3}$ m s^{-1}, while the 0.1 m-thick colmated layer around the lateral screen wall has the conductivity coefficient of $K = 10^{-4}$ m s^{-1}. Steady state conditions are assumed.

The examination of the accuracy includes the following: (1) influence of domain size (model radius) on solution accuracy; and (2) longitudinal mesh division effect on accuracy, when potential is constant or changes linearly along the cylinder's external surface.

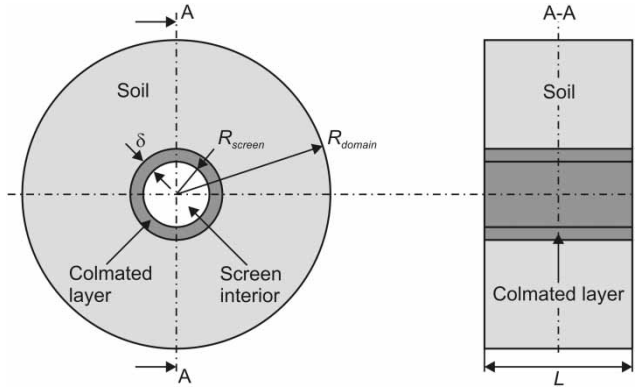

Figure 3 | Cylindrical model.

Effect of domain size

The domain size is changed by varying the external radius. The following radii are used (in m): 5, 10, 20, 30, 40, 50, 60, 70, 80, 90 and 100. The boundary conditions are: (1) potential 100 m at the outer boundary of the cylinder; and (2) potential 50 m within the inner cylinder.

The relative flow rate difference between 1D model and 3D model solutions, in terms of the domain size, is shown in Figure 4.

It is apparent that the domain size has a significant effect on solution accuracy. This is expected because the 1D model does not take into account the lateral screen interior as the external space with respect to the soil, and

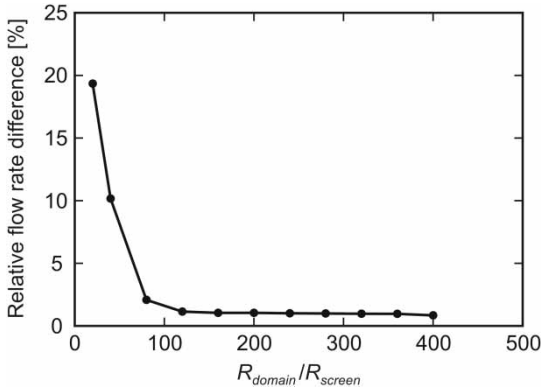

Figure 4 | Relative flow rate difference (in %) between 1D and 3D models in terms of domain size ($R_{\mathrm{domain}}/R_{\mathrm{screen}}$ ratio).

this difference between the two models is more pronounced for smaller R_{domain}/R_{screen} ratios.

Effect of longitudinal mesh division

Here we consider the domain whose external radius is equal to 50 m, with: (a) a constant potential along the cylinder axis equal to 100 m, and (b) a constant axial gradient along the external surface, with potentials 100 and 50 m at the front and back, respectively. In both cases the potential within the lateral screen is 50 m.

The relative error for several axial mesh densities (divisions 5, 10, 15 and 20) is shown in Figure 5. As expected (since the flow does not change along the cylinder axis), the error does not depend on axial mesh density.

In the case of an axial gradient, the relative error of the 1D model in terms of the axial mesh density is shown in Figure 6. It can be seen that now the error is slightly larger when the mesh is coarse in the axial direction. When the number of elements is increased, the error approaches the value of approximately 6%.

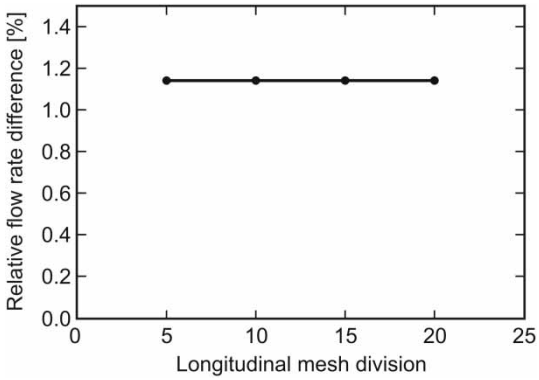

Figure 5 | Relative flow rate difference (in %) vs. longitudinal mesh division, constant potential along the cylinder.

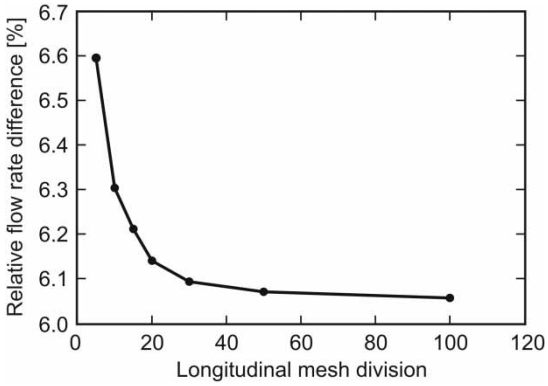

Figure 6 | Relative flow rate difference (in %) vs. number of elements in axial direction, case with axial potential gradient.

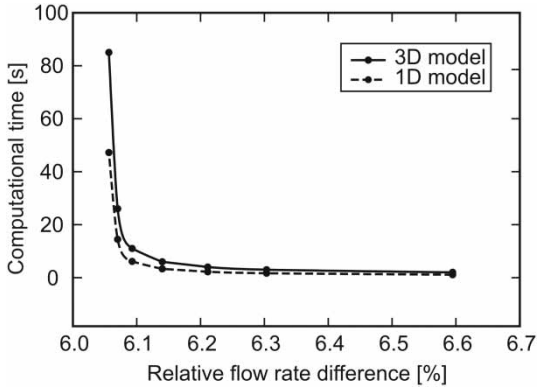

Figure 7 | Computational time (in s) vs. relative flow rate difference (in %), case with axial potential gradient; each point corresponds to relative flow rate difference in Figure 6.

Computational times are further compared for 3D and 1D models in case of the axial gradient. In Figure 7 a trade-off is shown between the accuracy and computational effort for these models. It can be seen that the difference in computational time is increased with the decrease of relative flow difference (i.e. increase of longitudinal mesh division) between the models.

Square-shaped (rectangular prism) domain

A prism-shaped flow domain of the lateral screen, with a 20×20 m square base (Figure 8) is now considered. It is assumed that the screen lies along the central prism axis, with the length of 15 m (L_{screen}) and 0.25 m in radius (R_{screen}). The screen is covered by the colmated layer of thickness 0.1 m (δ). The conductivity coefficients are $K = 10^{-3}$ and 10^{-4} m s^{-1} for the soil and the colmating layer, respectively. The longitudinal mesh division is taken to be the same for all cases shown below (1 element per meter). Steady state conditions are assumed.

In this example two effects on the 1D model solution accuracy are examined:

1. The effect of the longitudinal dimension L of the model, with the length of the screen L_{screen} being constant; and
2. The effect of the axial gradient.

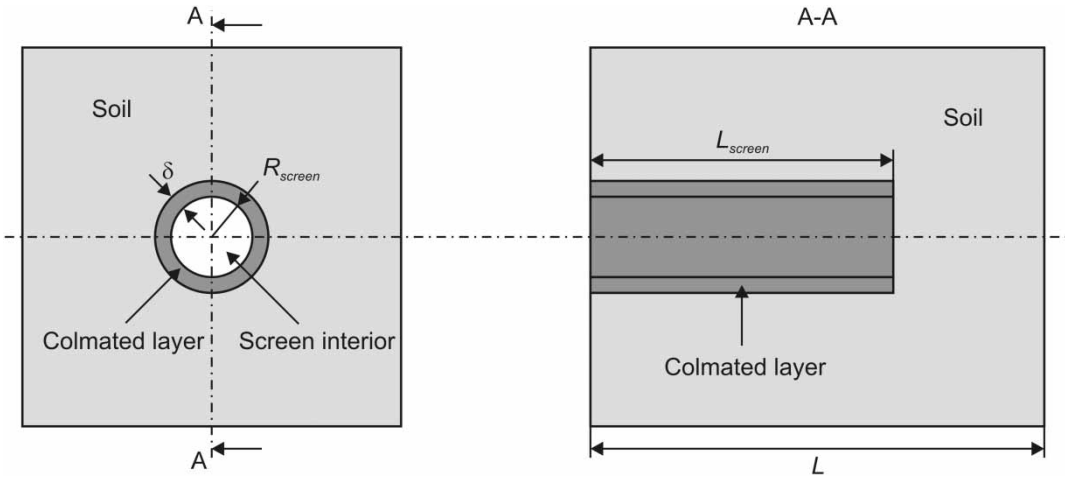

Figure 8 | Model of rectangular prism example.

Effect of the longitudinal dimension of the domain

Six models are used; their longitudinal dimensions (in m) are: 20, 30, 40, 50, 100 and 200. The boundary conditions are: (1) a potential equal to 10 m is specified on the prism side opposite to the lateral screen entrance; and (2) the potential within the interior of the screen is set at 5 m.

The relative flow rate difference between the 1D and 3D models for the six cases is shown in Figure 9. It is apparent that accuracy increases with the length of the model relative to the lateral screen length. The size effect is analogous to that shown in Example 1 (Figure 4).

Effect of longitudinal mesh division

Here the analysis was performed on a model whose length is $L = 20$ m. Other conditions were the same as above. The axial mesh density was varied and the flow rate was calculated for both 3D and 1D models.

Dependence of the relative error on the axial mesh density, expressed by the number of elements per meter, is shown in Figure 10. It is obvious that the relative error shows no noticeable sensitivity to longitudinal mesh division.

As in the case of cylindrical model, computational times for 3D and 1D models in case of the axial gradient are shown in Figure 11. The trade-off between the accuracy

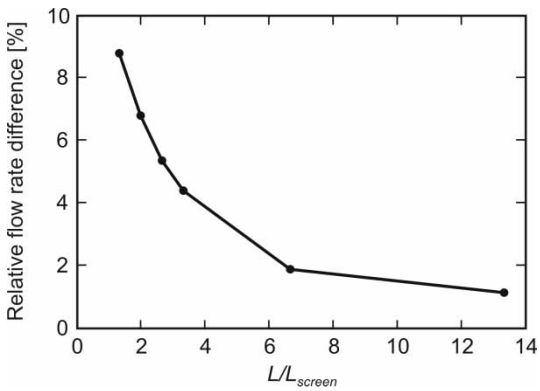

Figure 9 | Relative flow rate difference (in %) between 1D and 3D models in terms of the axial domain size (L/L_{screen}).

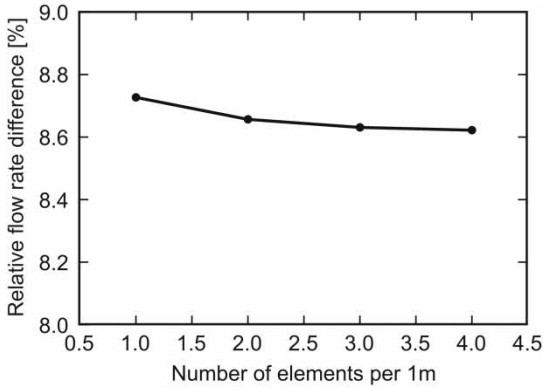

Figure 10 | Relative flow rate difference (in %) between 1D and 3D models in terms of longitudinal mesh division (number of elements per 1 m).

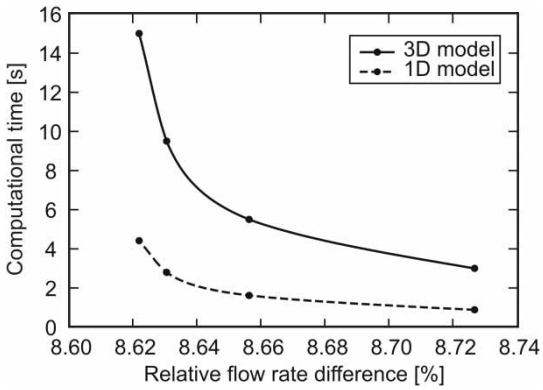

Figure 11 | Computational time (in s) vs. relative flow rate difference (in %), case with axial potential gradient; each point corresponds to relative flow rate difference in Figure 10.

and computational effort for these models has the same character as for the cylindrical model.

MODEL OF WELL RB-7, BELGRADE GROUNDWATER SOURCE

In this section a numerical model is presented for a part of the Belgrade Groundwater Source. Lateral screens are modeled using 1D FEs. We considered the RW (officially denoted as RB-7) which is located in the vicinity of the right bank of the Sava River. The numerical model includes the RW and the zones relevant to its operation: a portion of the river flow and a portion of the riverside area which holds neighboring wells. Position of RW RB-7, as well as horizontal positions and orientations of the well lateral screens and piezometers (P-1 and P-2), are shown in Figure 12.

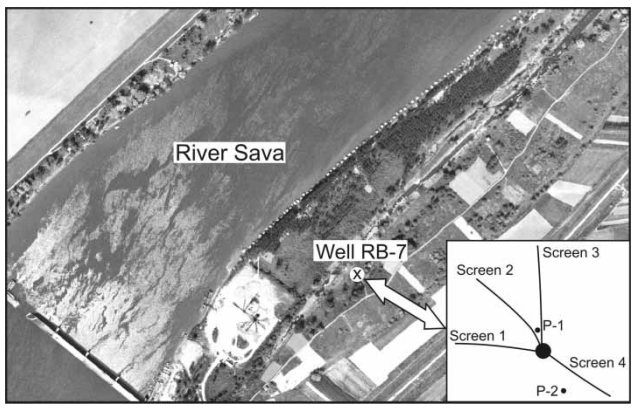

Figure 12 | Position of RW RB-7 and horizontal positions and orientations of the well lateral screens.

The natural setting aquifer was represented in the model by four water-bearing strata of different hydrogeological characteristics, obtained by measurements at several locations of the water source.

One of the most important benefits of computer modeling of the ground water flow in the screens vicinity is possibility to determine conductivities of colmated layers of existing RW lateral screens. This could be done through a procedure termed as model calibration. This procedure implies varying of conductivities of colmated layers of lateral screens until the actual groundwater potential, measured at the piezometers, fits water levels obtained by numerical calculation. On the other hand, calculated well discharge has to fit the flow rate variations recorded on a considered well during the test period. The model calibration may be very demanding because each change of colmated layer conductivity results in different diagrams of well flow rate and different diagrams of potential at piezometers. Therefore, model calibration implies a number of iterations.

Figure 13 shows diagrams of potential (measured and calculated) during the test period, at piezometers P-1 (Figure 13(a)) and P-2 (Figure 13(b)), after model calibration.

Diagrams of calculated and measured flow rate of the well RB-7 during test period are shown in Figure 14.

Figure 15 shows a section along Screen 3. The figure shows spacial distribution of water-bearing strata with the corresponding conductivities (in $m\,s^{-1}$), and calculated potential field represented by equipotential lines. The potential field corresponds to the end of the test period.

Model calibration provides representative values of the conductivity of RW lateral screens, which could be very useful in making decisions about future design of water source with RWs. More details about model calibration by using computer modeling, with 1D FEs for lateral screens, can be found in recent publication (Dimkic *et al.* 2011).

Considering the complexity of a real engineering problem, as the one shown above, enormous advantages regarding FE model generation, reduction in overall computational time (size of the model is huge and model calibration must be performed iteratively), and presentation of results, are obvious when our 3D–1D model is employed.

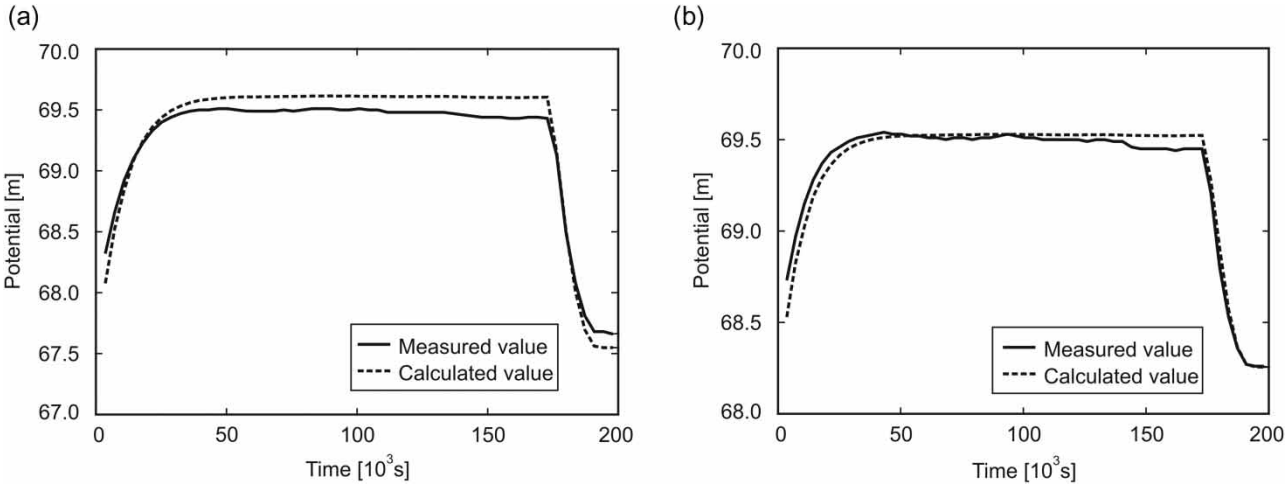

Figure 13 | Measured and calculated potential at piezometers: (a) P-1 and (b) P-2.

CONCLUSION

Continual monitoring of RW capacity is very important for adequate well exploitation (selection of the number and characteristics of the well laterals and the operating modes) and maintenance. Unlike in the case of conventional wells, groundwater flow in the vicinity of RWs is truly 3-dimensional. Detailed analyses of RWs regarding hydraulic losses at the entrance to the well lateral screens is very complex and often can only be evaluated by computer modeling. However, computer modeling of RWs using FE method can be very demanding. Due to excessively complex geometry of soil layers, irregular spreading of screens through the porous soil and extreme disproportion between model dimensions and lateral screens dimensions, generation of a full 3D mesh requires significant effort to track all these conditions.

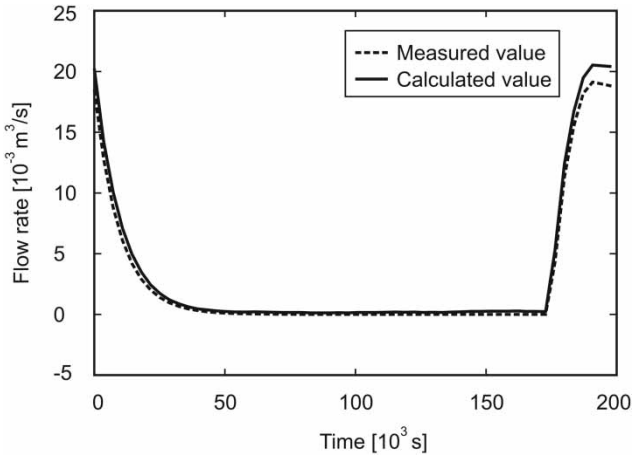

Figure 14 | Measured and calculated values of well flow rate during test period.

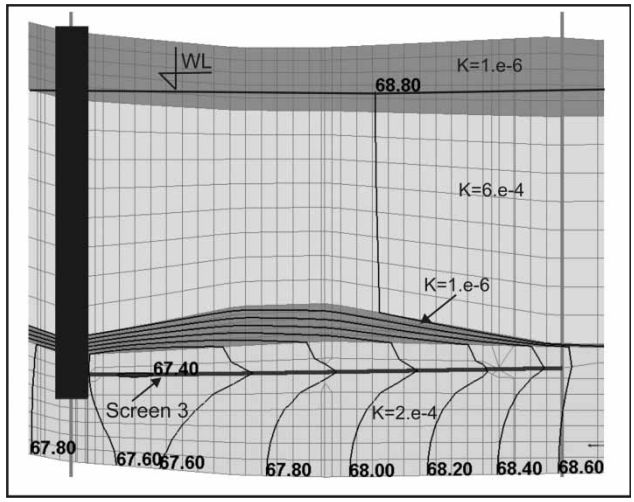

Figure 15 | Spacial distribution of water-bearing strata and equipotential lines at the end of test period.

In this paper we have introduced a simple and straightforward novel concept for 1D FE modeling of RW lateral screens, which is computationally efficient, user friendly and elegant. The proposed concept was verified by analyzing solution accuracy on typical examples. The main parameter affecting the accuracy of the 1D screen model is the flow domain size with respect to lateral screen dimensions. Accuracy sharply increases as the domain size

increases. Since in the real water supply systems size of the flow domain is huge with respect to the screen dimensions, it can be concluded that this 1D screen model provides reliable results. Furthermore, solution error due to 1D representation of lateral screens is also acceptable when compared with the overall accuracy of water supply system models which rely on many approximations, such as geometry of soil layers, material characteristics, etc. In summary, this concept offers significant comfort in creating FE models of large water supply systems, results are easily displayed, and accuracy is acceptable for practical applications.

ACKNOWLEDGEMENT

Research presented in this paper was supported by Serbian Ministry of Science and Technology, Grant III-41007.

REFERENCES

Bakker, M., Kelson, V. A. & Luther, K. H. 2005 Multi-layer analytic element modeling of radial collector wells. *Ground Water* **43**, 926–934.

Bischoff, H. 1981 An integral equation method to solve three dimensional flow to drainage systems. *Applied Mathematical Modeling* **5**, 399–404.

Chen, C., Wan, J. & Zhan, H. 2003 Theoretical and experimental studies of coupled seepage-pipe flow to a horizontal well. *Journal of Hydrology* **281**, 159–171.

Chen, Z. & Zhang, Y. 2009 Well flow models for various numerical methods. *International Journal of Numerical Analysis and Modeling* **6**, 375–388.

Dimkic, M. & Pusic, M. 2008 Well-ageing indicators, with special reference to the Belgrade groundwater source. In: *Groundwater Management in Large River Basins* (M. Dimkic, ed.). IWA Publishing, London, Ch. 4.7.

Dimkic, M., Filipovic, N., Stojanovic, B., Rankovic, V., Isailovic, V., Otasevic, L., Ivanovic, M., Pusic, M. & Kojic, M. 2009 Lizza – pre- and post-processor for modeling of underground water flow with Ranney wells. BioIRC Kragujevac and Institute for Development of Water Resources 'Jaroslav Cerni', Serbia.

Dimkic, M., Krstic, M., Filipovic, N., Stojanovic, B., Rankovic, V., Otasevic, L., Ivanovic, M., Nedeljkovic, M., Trickovic, M., Pusic, M., Boreli-Zdravkovic, Dj., Djuric, D. & Kojic, M. 2007a Comparison of different configurations of Ranney Wells using finite element modeling. *Journal of the Serbian Society for Computational Mechanics* **1**, 144–153.

Dimkic, M., Tausanovic, V., Pusic, M., Boreli-Zdravkovic, Dj., Djuric, D., Slimak, T., Petkovic, A., Obradovic, V. & Babic, R. 2007b Belgrade Groundwater Source, Condition and Possible Development Directions. *Regional IWA Conference On Groundwater Management in the Danube River Basin and other Large River Basins*, Belgrade, Serbia, pp. 137–150.

Dimkic, M., Pusic, M., Vidovic, D., Isailovic, V., Majkic, B. & Filipovic, N. 2011 Numerical model assessment of radial-well aging. *Journal of Computing in Civil Engineering* **25**, 43–49.

Eberts, S. M. & Bair, E. S. 1990 Simulated effects of quarry dewatering near a municipal well field. *Ground Water* **28**, 37–47.

Haitjema, H. M., Kuzin, S., Kelson, V. & Abrams, D. 2010 Modeling flow into horizontal wells in a Dupuit-Forchheimer model. *Ground Water* **48**, 878–883.

Huisman, L. 1972 *Groundwater Recovery*. MacMillan, London, UK.

Kojic, M., Filipovic, N., Slavkovic, R., Zivkovic, M. & Grujovic, N. 1998 *PAK-P Finite Element Program for Modeling of Underground Water Flow and Seepage*. Faculty of Mech. Eng. Univ. of Kragujevac, Kragujevac, Serbia.

Luther, K. H. & Haitjema, H. M. 2000 Approximate analytic solutions to unconfined 3D groundwater flow within 2D regional models. *Journal Hydrology* **229**, 101–117.

Ophori, D. U. & Farvolden, R. N. 1985 A hydraulic trap for preventing collector well contamination: a case study. *Ground Water* **23**, 600–610.

Pusic, M. & Dimkic, M. 2008 Mathematical modeling, a tool for groundwater regime management. In: *Groundwater Management in Large River Basins* (M. Dimkic, ed.). IWA Publishing, London, Ch. 5.

Ray, C., Grischek, T., Schubert, J., Wang, J. Z. & Speth, T. 2002 A perspective of riverbank filtration. *Journal of American Water Works Association* **94**, 149–160.

Steward, D. R. & Jin, W. 2001 Gaining and losing sections of horizontal wells. *Water Resources Research* **37**, 2677–2685.

Strack, O. D. L. 1989 *Groundwater Mechanics*. Prentice Hall, Englewood Cliffs, New Jersey. Available from: http://www.strackconsulting.com.

Zhan, H. & Park, E. 2003 Horizontal well hydraulics in leaky aquifers. *Journal of Hydrology* **281**, 129–146.

Zhan, H. & Zlotnik, V. A. 2002 Groundwater flow to a horizontal or slanted well in an unconfined aquifer. *Water Resources Research* **38**, 131–1311.

First received 11 January 2012; accepted in revised form 29 June 2012. Available online 10 October 2012